Hydrogen Bond Rearrangements and Interconversions of H + (CH 3 OH) 4 H 2 O Cluster Isomers †

ARTICLE *in* THE JOURNAL OF PHYSICAL CHEMISTRY A · NOVEMBER 2002

Impact Factor: 2.69 · DOI: 10.1021/jp020537u

4 AUTHORS, INCLUDING:

Jyh-Chiang Jiang
National Taiwan University of Science and Te…

173 PUBLICATIONS **2,576** CITATIONS

SEE PROFILE

Hydrogen Bond Rearrangements and Interconversions of $H^+(CH_3OH)_4H_2O$ Cluster Isomers†

J. C. Jiang,‡ C. Chaudhuri,§ Y. T. Lee,§,⊥ and H.-C. Chang*,§

Department of Chemical Engineering, National Taiwan University of Science and Technology, Taipei, Taiwan 106, R.O.C., Institute of Atomic and Molecular Sciences, Academia Sinica, P.O. Box 23-166, Taipei, Taiwan 106, R.O.C., and Department of Chemistry, National Taiwan University, Taipei, Taiwan 106, R.O.C.

Received: February 26, 2002; In Final Form: May 28, 2002

Rearrangement of hydrogen bonds in the protonated methanol−water cluster ion $H^+(CH_3OH)_4H_2O$ is analyzed. The analysis, based on ab initio calculations performed at the B3LYP/aug-cc-pVTZ//6-31+G* and MP4/6-311+G*//B3LYP/6-31+G* levels of computation, provides information about potential minima, transition states, and pathways for the hydrogen bond rearrangement processes. Results of the analysis are compared systematically to the experimental measurements for $H^+(CH_3OH)_4H_2O$, where two distinct charge-centered (H_3O^+ and $CH_3OH_2^+$) isomers have been identified in a supersonic expansion by fragment-dependent vibrational predissociation spectroscopy (Chaudhuri et al. *J. Chem. Phys.* **2000**, *112*, 7279). Revealed by the calculations, the lowest energy pathway for the transition from an open noncyclic hydronium-centered isomer $[H_3O^+(CH_3OH)_4]$ to a linear methyloxoium-centered isomer $[CH_3OH_2^+(CH_3OH)_3H_2O]$ involves three stable intermediates and four transition states. The transition can go through either all four-membered ring isomers or a mixture of four-membered and five-membered ring intermediates. The latter is an energetically more favorable process because of less strain involved in the five-membered ring formation. A barrier height of <2.5 kcal/mol (after zero-point energy corrections) is predicted, suggesting that rapid interconversions among different isomers can occur at room temperature for this particular cluster cation.

I. Introduction

Rearrangement of hydrogen bonds (HB) predominates the dynamics of ion hydration in aqueous solutions.[1,2] It involves making, breaking, and reforming of hydrogen bonds between adjacent pairs of water molecules and often takes place on the time scale of picoseconds with a barrier height of ∼3 kcal/mol.[3] The process may find analogies in biological systems where folding, unfolding, and refolding of proteins[4,5] are also associated with hydrogen bond rearrangements. Inspired by the fundamental importance of these processes, considerable efforts have been made to understand the HB reorganization dynamics using molecular clusters as the prototypical systems. Wales[6] theoretically analyzed the HB rearrangements derived from hydrogen tunneling in neutral water clusters investigated by far-infrared vibration−rotation tunneling spectroscopy.[7] The tunneling motions can either go through a single flipping process or follow a bifurcation pathway for $(H_2O)_n$ of $n = 3$ and 5. Examination of the tunneling components has led Saykally and co-workers[8] to obtain the first molecular picture of hydrogen bond breaking dynamics in the translational and librational vibration regions of liquid water. Extending the studies to larger clusters $(H_2O)_8$ and $(H_2O)_{20}$, Wales and Ohmine[9] illustrated a wider range of water reorganization processes. The illustration, yielded by molecular dynamics simulations using parametrized pair potentials for rigid water monomers, provides new insights into the melting transitions of nanometer-sized water clusters.

Theoretical analysis of water clusters in protonated forms also reveals intriguing tunneling processes involving the extra proton.[10] The tunneling, while only experimentally observed for $H^+(H_2O)_2$,[11] may go through two pathways, corresponding to either monomer inversion or internal rotation of one of the two water subunits. Employing basin-hopping Monte Carlo simulations and empirical potentials, Singer et al.[12] theoretically analyzed the topology of $H^+(H_2O)_8$ and $H^+(H_2O)_{16}$ as a function of temperature. They concluded that the treelike topology with chains of water molecules emanating from a hydronium ion core is favored by Gibbs free energies at room temperature for both clusters. Their conclusion is in qualitatively good agreement with the experimental observations for $H^+(H_2O)_{5-8}$ by Jiang et al.[13] using vibrational predissociation spectroscopy.

The simplest HB rearrangement, if one envisions, is a process involving making and breaking of a single hydrogen bond. The process has been closely examined in the study of the transition between cyclic and noncyclic isomers induced either by thermal annealing or by collisional activation of $NH_4^+(H_2O)_5$ (ref 14) and $H^+(CH_3OH)_5$.[15] The two cluster systems accordingly display characteristic hydrogen-bonded OH stretching vibrations at ∼3500 cm^{-1}, allowing comprehensive investigations of the underlying HB rearrangement dynamics to be made using infrared spectroscopic methods. A more complex form of the HB rearrangement, which may give rise to loss of the water molecule sandwiched between two dimethyl ether subunits, has also been detected for $H^+[(CH_3)_2O]_2(H_2O)$.[16] Knowledge of the mechanism of this rearrangement is deduced from a temperature-

† Part of the special issue "R. Stephen Berry Festschrift".

* Corresponding author. E-mail: hcchang@po.iams.sinica.edu.tw.
‡ Department of Chemical Engineering, National Taiwan University of Science and Technology.
§ Institute of Atomic and Molecular Sciences, Academia Sinica.
⊥ Department of Chemistry, National Taiwan University.

10.1021/jp020537u CCC: $22.00
Published on Web 08/24/2002

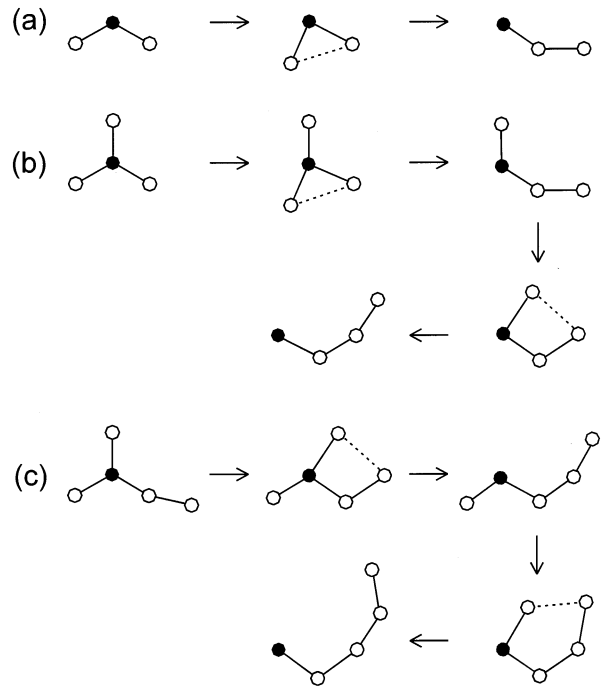

Figure 1. Schematic presentation of the hydrogen bond rearrangements of water-containing trimers (a), tetramers (b), and pentamers (c). The solid circle denotes H_2O and the open circles denote $(CH_3)_2O$ or CH_3OH molecules.

dependent measurement of the free-OH stretch spectra of H_2O at 150−200 K. A schematic diagram of such a HB rearrangement process is illustrated in Figure 1a, with the solid circle denoting H_2O and the open circles denoting the $(CH_3)_2O$ molecules.

To continue the research along this line, we have recently conducted a detailed analysis for the HB rearrangement in protonated mixed methanol−water clusters using $H^+(CH_3OH)_n(H_2O)$ as the benchmark system. With CH_3OH substituting $(CH_3)_2O$ in Figure 1a, more complex HB rearrangement schemes emerge at $n > 2$. As illustrated pictorially in Figure 1, the expected HB rearrangements for these clusters $[H^+(CH_3OH)_n(H_2O)]$ with a size of $n = 2-4$ can involve both ring opening and closing or, more specifically, formation and deformation of the three-membered, four-membered, and five-membered ring isomers as the intermediates. It is of interest to note that such illustrated HB rearrangements will lead not only to change of the clusters' structures but also to transport of the excess proton within the clusters to form either H_3O^+-centered or $CH_3OH_2^+$-centered isomers. Furthermore, in the course of this interconversion [denoted as $H_3O^+(CH_3OH)_n \leftrightarrow CH_3OH_2^+(CH_3OH)_{n-1}H_2O$], the water molecule will migrate sequentially from the center as an ion core to the cluster's surface as a neutral subunit (and vice versa). It features migration of a single water molecule out of (and into) a protonated methanol "cage".

Previously,[17] we reported results of our attempts to observe these intriguing HB rearrangements using vibrational predissociation spectroscopy in combination with density functional theory calculations. Both H_3O^+-centered and $CH_3OH_2^+$-centered treelike isomers have been experimentally identified for $H^+(CH_3OH)_4(H_2O)$; however, the thorough dynamical mechanism by which these isomers are interconverted is still not known. This paper presents a full theoretical analysis, together with experimental results, for the mechanism of the interconversion, which contains knowledge of potential minima and transition states as well as pathways for this protonated methanol−water cluster.

II. Experiments

Experimental spectra are acquired with use of a vibrational predissociation ion trap mass spectrometer and a pulsed infrared laser system described previously.[14] We generated the mixed methanol−water cluster ions from a supersonic expansion of corona-discharged CH_3OH/H_2O vapor seeded in pure H_2. The expansion proceeded through a room-temperature nozzle with an orifice diameter of $\sim 75\ \mu$m at a backing pressure in the range of 30−100 Torr. Hydrogen was used here both as the carrier gas for efficient jet cooling and as a protonation source according to the following mechanism and the associated energetics,

$$H_2 + e^- \rightarrow H_2^+ + 2e^-$$

$$H_2^+ + H_2 \rightarrow H_3^+ + H \qquad \Delta H^\circ = -13.3 \text{ kcal/mol}$$

$$H_3^+ + CH_3OH \rightarrow H_2 + CH_3OH_2^+ \qquad \Delta H^\circ = -79.4 \text{ kcal/mol}$$

$$H_3^+ + H_2O \rightarrow H_2 + H_3O^+ \qquad \Delta H^\circ = -64.3 \text{ kcal/mol}$$

The typical corona discharge current used in this experiment was $\sim 250\ \mu$A, which produced cluster ions with a steady current of ~60 pA measured by a Faraday cup at a distance of 50 cm from the source cell.

Generated by the molecular beam expansion, the cluster ions of interest $[H^+(CH_3OH)_4H_2O]$ were first mass-selected by a magnet sector and then stored in an octopole ion trap for infrared laser excitation. A quadrupole mass filter monitored the excitation consequence and selectively detected the resulting photofragments, either $H^+(CH_3OH)_4$ or $H^+(CH_3OH)_3H_2O$. Fragment-dependent vibrational predissociation spectra resulted from recording of the ion signals as a function of laser frequency. With a dissociation energy of ~13 kcal/mol,[18] the $H^+(CH_3OH)_4H_2O$ ion can be fragmented at the expense of internal energy upon absorption of the infrared laser photons at 2800−3800 cm^{-1} (or 8−11 kcal/mol in energy) via a one-photon process.

For the protonated mixed methanol−water clusters $H^+(CH_3OH)_n(H_2O)_m$,[18−25] there are two possible pathways for the dissociation to occur, either via water loss (denoted as W-loss) or via methanol loss (denoted as M-loss). Garvey and co-workers[24] have studied extensively the mass-selected cluster ions of $m = 1$, and found that the channel involving loss of a single water molecule dominates at $n \leq 8$, whereas loss of multiple CH_3OH molecules is the favored decomposition channel at $n \geq 9$. This indicates the existence of a magic cluster isomer for $H^+(CH_3OH)_9(H_2O)$. They assign the structure of this isomer to a symmetrically solvated H_3O^+ entity by the methanol molecules. Despite that CH_3OH has a proton affinity significantly higher than that of H_2O,[26] the latter can still take the proton and behave as the central ion in a cage composed of nine interconnected methanol molecules.

On the basis of all prior studies,[18−25] we expect that both the W-loss and M-loss fragmentation channels are open and detectable for $H^+(CH_3OH)_4(H_2O)$. According to the thermochemical measurements of Meot-Ner,[18] the respective stepwise dissociation energies involved in these two channels are

$$H^+(CH_3OH)_4H_2O \rightarrow H^+(CH_3OH)_3H_2O + CH_3OH \qquad \Delta H^\circ(\text{M}) = 14.4 \text{ kcal/mol}$$

$$H^+(CH_3OH)_4H_2O \rightarrow H^+(CH_3OH)_4 + H_2O$$
$$\Delta H°(W) = 12.1 \text{ kcal/mol}$$

which suggest a branching ratio of $\exp[-\Delta H°(W)/k_BT]$: $\exp[-\Delta H°(\mathbf{M})/k_BT] = 800{:}1$ at 170 K, strongly favoring the W-loss channel. Such a preferential loss of water is expected from the proton affinity difference of PA(**M**) − PA(**W**) = 15.1 kcal/mol between CH_3OH and H_2O[26] and is in line with the observations of Lyktey et al.[24] who detected a negligible loss of methanol in the metastable decomposition of $H^+(CH_3OH)_4(H_2O)$. In our experiments, we found that the M-loss channel is less accessible than the W-loss channel by roughly a factor of 30, determined from the fraction of the photofragments being produced. We attribute the discrepancy between our observation and the result of Garvey group[24] to the likelihood that the relative abundance of isomers produced in the molecular beams differs because different methods are used for the cluster synthesis.

One unique feature of the mixed methanol−water cluster ions is that they can be centered either with $CH_3OH_2^+$ or with H_3O^+, conditional on the structure and size of the cluster.[18−25] Interestingly, one can differentiate these cluster isomers by collection of the vibrational predissociation spectra, which are governed by either W-loss or M-loss. For $H^+(CH_3OH)_4(H_2O)$, an H_3O^+-centered structure may preferentially promote loss of the methanol molecule whereas a $CH_3OH_2^+$-centered structure promotes loss of the water unit. A diagram illustrating such an intriguing selective fragmentation behavior for this cluster is shown in Figure 2, with use of three stable open chain isomers **WM4I**−**WM4III** as the example. While these three isomers are apparently similar in structure, they actually differ in the role the water molecule plays within the cluster. The water molecule can either act as an ion core (H_3O^+) in **WM4I** or as a solvent molecule situated on the first-solvation shell in **WM4II** or on the second-solvation shell of the $CH_3OH_2^+$ ion in **WM4III**. The single water molecule thus serves as a "tag" for monitoring the HB rearrangement processes in this cluster.

In dissociation of cluster isomers **WM4I**−**WM4III**, the two most likely forms of the products from the M-loss channel are **WM3I** and **WM3II** (structures depicted in Figure 2). According to the B3LYP/aug-cc-pVTZ//6-31+G* level of computation (as to be discussed in section III), they contain about the same amount of total interaction energy as

$$H_3O^+ + 3CH_3OH \rightarrow \textbf{WM3I} \text{ (or } \textbf{WM3II})$$
$$\Delta H_n^{298} = -64.2 \text{ kcal/mol}$$

The difference in ΔH_n^{298} between these two isomers is 0.1 kcal/mol, essentially within the limit of our computational errors. For the W-loss channel, the dissociation product is **M4I** (cf. Figure 2),[15] which contains a total clustering energy of

$$CH_3OH_2^+ + 3CH_3OH \rightarrow \textbf{M4I},$$
$$\Delta H_n^{298} = -66.2 \text{ kcal/mol}$$

It suggests a preferential loss of water by about 2 kcal/mol upon vibrational excitation of $H^+(CH_3OH)_4H_2O$. Hence, from the energetic point of view, the excitation should lead to preferential loss of water in dissociation of both isomers **WM4I** and **WM4III**, since it is the lowest energy pathway. However, from a kinetics point of view, the water loss from **WM4I** is a highly unfavorable process, since the isomer contains an H_3O^+ ion core fully surrounded by more than one layer of methanol molecules and three hydrogen bonds must be broken in order to dissociate.

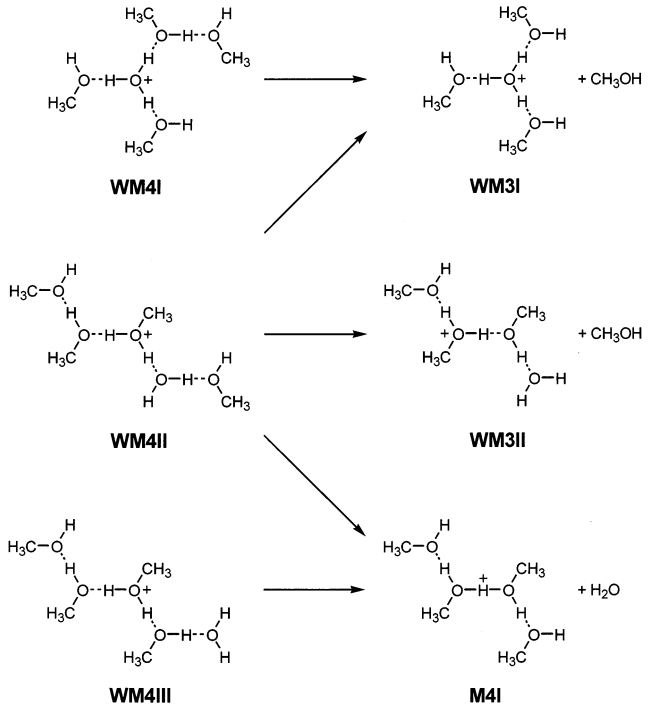

Figure 2. Selective fragmentation of three stable open chain isomers, **WM4I**−**WM4III**, yielding three possible products **WM3I**, **WM3II,** and **M4I**.

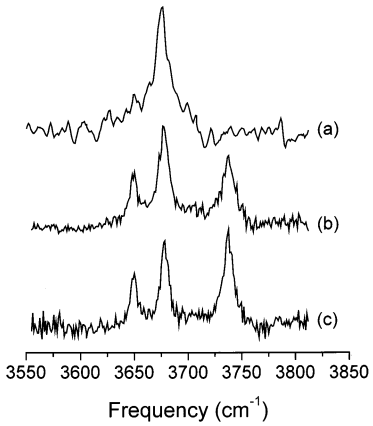

Figure 3. Power-normalized vibrational predissociation spectra of $H^+(CH_3OH)_4H_2O$ generated by a supersonic expansion with a backing pressure of 30 Torr [(a) and (b)] and 100 Torr (c) behind a room-temperature nozzle. The spectra were obtained by monitoring either methanol loss (a) or water loss [(b) and (c)] upon excitation of the cluster in the free-OH stretching region.

Figure 3 reproduces the spectra of $H^+(CH_3OH)_4H_2O$ in the free-OH stretching region, obtained by scanning the frequency from 3500 to 3800 cm^{-1} and monitoring either (a) M-loss or (b) W-loss. As noted, the spectra markedly differ from each other; only a single band is recorded at 3677 cm^{-1} in Figure 3a, whereas three bands are recorded at 3649, 3677, and 3737 cm^{-1} in Figure 3b. The spectral features can be reasonably assigned to (a) the free-OH stretches of the neutral methanol molecules and (b) the symmetric and asymmetric free-OH stretches of water, acting as a single proton acceptor in the outer solvation shell (cf. Table 2 for detailed assignments). The marked differences between the spectra in parts a and b of Figure 3 clearly indicate that at least two distinct types of structural isomers are present in the supersonic expansion. The isomers that are most likely to be responsible for the experimental spectra are **WM4I** and **WM4III** (cf. Figure 2), as assigned previously.[17]

TABLE 1: DFT Calculated Total Energies (kcal/mol) of the Clustering via Channel (I) $H_3O^+ + 4CH_3OH \rightarrow H^+(CH_3OH)_4H_2O$ and Channel (II) $CH_3OH_2^+ + 3CH_3OH + H_2O \rightarrow H^+(CH_3OH)_4H_2O$ and Their Comparison with Experimental Values at 298 K

	calcd I (II)[a]				exptl I (II)[b]	
isomers[c]	$-\Delta E_n$	$-\Delta H_n^{298}$	$-\Delta G_n^{298}$	$-\Delta G_n^{170}$	$-\Delta H_n°$	$-\Delta G_n°$
WM4I	89.7 (74.6)	90.9 (74.9)	56.7 (41.3)	71.4 (55.8)	96.7 (81.6)	64.2 (48.7)
WM4II	90.0 (74.9)	91.2 (75.2)	56.5 (41.1)	71.4 (55.8)		
WM4III	90.5 (75.4)	91.5 (75.5)	57.2 (41.8)	71.9 (56.3)		
WM4IV	89.3 (74.3)	91.1 (75.1)	53.7 (38.3)	69.8 (54.1)		
WM4V	88.6 (73.5)	90.4 (74.4)	52.2 (36.8)	68.6 (53.0)		
WM4VI	88.0 (72.9)	89.9 (73.9)	51.7 (36.3)	68.0 (52.4)		
WM4VII	89.0 (73.9)	90.8 (74.8)	52.9 (37.5)	69.1 (53.5)		
WM4VIII	89.1 (74.0)	90.6 (74.6)	52.8 (37.4)	69.0 (53.4)		
WM4IX	86.4 (71.3)	87.3 (71.3)	49.9 (34.5)	66.1 (50.7)		
WM4X	90.2 (75.1)	92.0 (76.0)	53.3 (37.9)	69.7 (54.3)		
WM4XI	88.6 (73.5)	90.5 (74.5)	52.2 (36.8)	68.4 (53.0)		
WM4XII	88.9 (73.8)	90.8 (74.8)	51.9 (36.5)	68.4 (53.0)		
WM4XIII	90.4 (75.3)	92.0 (76.0)	54.3 (38.9)	70.2 (54.8)		

[a] Using the B3LYP/aug-cc-pVTZ//6-31+G* level of computation with zero-point vibrational energies corrected. [b] Calculated from refs 18 and 26 using the proton affinity difference PA(M) − PA(W) = 15.1 kcal/mol and the gas basicity difference GB(M) − GB(W) = 15.5 kcal/mol. [c] Structures illustrated in Figure 4.

TABLE 2: Frequencies, Bandwidths (cm^{-1}), and Assignments of the Observed OH Stretch Bands in the Vibrational Predissociation Spectra of $H^+(CH_3OH)_4(H_2O)$

obsd freq	fwhm[a]	calcd freq[b]	isomers[c]	assignments[d]
3737	12	3741	**WM4III**	a-OH_2 of 2° H_2O
3677	10	3656, 3666, 3673	**WM4I**	f-OH of 1° CH_3OH & 2° CH_3OH
		3668	**WM4III**	f-OH of 2° CH_3OH
3649	9	3637	**WM4III**	s-OH_2 of 2° H_2O
3336	52	3262	**WM4I**	b-OH of 1° CH_3OH
		3362	**WM4III**	b-OH of 1° CH_3OH
3073	250	3235	**WM4III**	b-OH of 1° CH_3OH

[a] Full width at half-maximum (fwhm) obtained by band deconvolution. [b] Frequencies scaled by 0.973 for all OH stretches. [c] Structures illustrated in Figure 4. [d] Notations follow that of ref 17.

The isomer **WM4II**, is not identified since the fingerprint of this species, namely, the 2-coordinated free-OH stretch of H_2O at ~3710 cm^{-1},[25] is not found in the experimental spectra.

The absence of the free-OH stretch absorption bands of H_2O in the M-loss spectrum (Figure 3a) leads us to a nearly conclusive identification of the H_3O^+-centered isomer (**WM4I**), since this isomer is least likely to lose its water molecule upon vibrational excitation. To further identify the existence of both **WM4I** and **WM4III** in the beam, a temperature-dependent measurement of the W-loss spectrum was conducted and the results are compared in parts b and c of Figure 3. As shown, the peak intensity of the 3677 cm^{-1} band is significantly lowered relative to that of the 3649 and 3737 cm^{-1} bands, when the backing pressure behind the corona-discharge nozzle is increased by about 3-fold (30 to 100 Torr). A measurement of the metastable decomposition rate[27] of W-loss for the clusters in the octopole ion trap revealed a temperature change of only 10 K from (b) to (c) in Figure 3. The change is folded with an estimated absolute temperature of 170 K, obtained by fitting the measured evaporative rate to a Klots evaporative ensemble model.[28] While such an estimation may not be exact, it provides a good reference for the temperature variation of the clusters in a supersonic expansion with steady ion currents produced by a stable corona discharge.

One may attribute the spectral changes in parts b and c of Figure 3 to the change in relative abundance of isomers **WM4I** versus **WM4III** with beam temperature. However, it may also arise from an increase in unimolecular loss of water from isomers **WM4I** and **WM4II** as the beam temperature is raised. Observation of the water loss from the vibrationally excited **WM4I** would clearly be a surprise, since three hydrogen bonds are needed to rupture.[24] For **WM4I**, to have the water loss, the dissociation must go through a chain process of intracluster hydrogen bond rearrangements before the W-loss fragmentation can occur. The possibility for the isomeric interconversion leading to the water loss is explored in the following theoretical section.

III. Calculations

Ab initio calculations are carried out using the commercial Gaussian 98 program.[29] We employed density functional theory (DFT) calculations, with the hybrid B3LYP method and the 6-31+G* basis set, to provide fully optimized geometries and vibrational frequencies of the cluster ions.[30] To correct vibrational anharmonicity, the calculated harmonic frequencies were scaled by 0.973 for both the free- and hydrogen-bonded-OH stretches of H_2O and CH_3OH. Single-point calculations were conducted with use of a larger basis set (aug-cc-pVTZ)[31] for the total interaction energies based on the potential minima located by B3LYP/6-31+G* for various cluster isomers. Results of the hybrid calculations (denoted as B3LYP/aug-cc-pVTZ//6-31+G*) are compared to experimental measurements as shown in Table 1. No correction is made for the basis set superposition error (BSSE) when using the aug-cc-pVTZ basis set.[31]

The B3LYP/6-31+G* level of calculation was also applied to search for transition states in the interconversion between cluster isomers **WM4I** and **WM4III**. First-order saddle points were located using the Berny transition-state algorithm.[29] To make better assessment of the energies of the transition states, single-point calculations at the MP4(SDQ)/6-311+G* level were performed. The validity of this method (denoted as MP4/6-311+G*//B3LYP/6-31+G*) was verified from a comparative study of the calculated results with those of CCSD/6-311+G*//B3LYP/6-31+G* for smaller clusters $[H^+(CH_3OH)_{2,3}H_2O]$ as will be presented in detail elsewhere.[32]

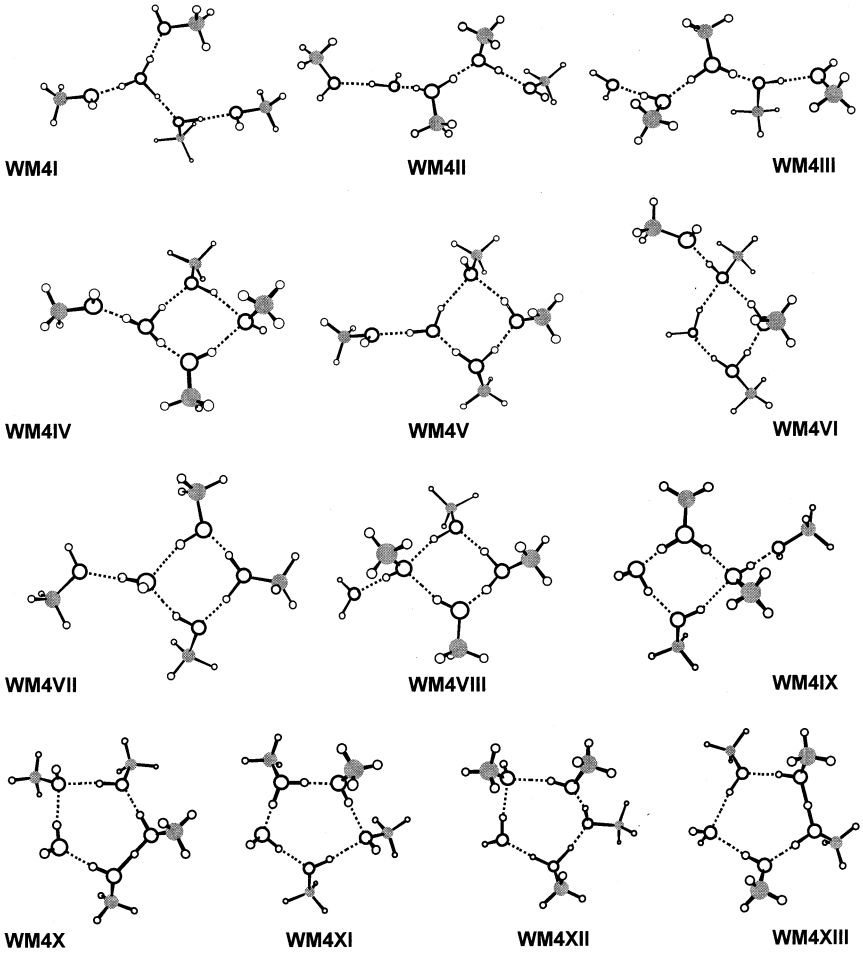

Figure 4. DFT-optimized geometries of $H^+(CH_3OH)_4H_2O$ isomers. The C, O, and H atoms are denoted by large shaded, large open, and small open circles, respectively. Note that, among the 13 low-energy species, **WM4I** and **WM4IV** are the only two isomers containing an H_3O^+ ion core.

Figure 4 depicts 13 isomeric structures of $H^+(CH_3OH)_4H_2O$ obtained from the DFT calculations.[33] They can exist in either cyclic or noncyclic forms, all lying in an energy range of ±2 kcal/mol (ΔE_n in Table 1). Notably, most of them are $CH_3OH_2^+$-centered, except isomers **WM4I** and **WM4IV**, which contain an H_3O^+ ion core. The predominance of the $CH_3OH_2^+$-centered forms can be understood as a result of CH_3OH having a higher proton affinity than H_2O and, therefore, can preferentially take the proton. For isomers **WM4I**−**WM4III**, they differ from one another primarily on the location of the water molecule, whereas for the six four-membered ring structures (**WM4IV**−**WM4IX**), they are distinct from each other on the position, orientation, and status (donor/acceptor) of the single water molecule either included in or bound to the 4-folded rings. Similar to the case of $H^+(H_2O)_n(CH_3OH)$ (ref 25) and $H^+(CH_3OH)_5$,[15] all the ring isomers are significantly higher in Gibbs free energy (Table 1) than the open noncyclic isomers at a cluster temperature of 170 K. Therefore, they are not expected to exist in a substantial amount in the present corona-discharged supersonic expansion. Aside from the four-membered ring isomers, the molecules can rearrange themselves to form five-membered rings (**WMX**−**WMXIII**), which closely resemble those of the pure methanol pentamers described in our earlier publications.[15] Despite that the bond strain is significantly reduced in the five-membered ring formation, these isomers remain unlikely to prevail in the supersonic expansion at 170 K (cf. ΔG_n[170] in Table 1) due to the entropy effect.

The prediction that ring isomers should not prevail in the beam is consistent with our experimental observations (Figure 5) that the fingerprints, namely, the hydrogen-bonded OH stretches at 3450−3550 cm^{-1}, of these isomers are not identified in the spectrum. Figure 5 compares the DFT-calculated stick diagrams of six representative isomers with the W-loss spectrum of $H^+(CH_3OH)_4H_2O$ in both the free- and hydrogen-bonded-OH stretch regions. Hindered by the severe band broadening of the spectrum, the only feature that can be clearly assigned in the frequency range of 2800−3600 cm^{-1} is the band centered at 3336 cm^{-1}, ascribable to the bonded-OH stretches of either H_2O or CH_3OH situated in the first solvation shell (cf. Table 2). We found no evidence for the ring formation of these cluster isomers.

In analysis of the isomeric interconversion, we identify a low-energy pathway for the formation of **WM4III** from the H_3O^+-centered isomer **WM4I**. It is composed of three stable isomers as the intermediate states, **WM4I** → **WM4V** → **WM4II** → **WM4XII** → **WM4III**, leading to the final dissociation products **M4I** and H_2O (cf. Figure 2). Note that each step of the conversion involves one transition state and thus the whole pathway samples four transition states, **TS1**−**TS4**. Figure 6 illustrates the result of a computational scan along the isomerization potential energy surfaces for the multiple-step barriers using the MP4(SDQ)/6-311+G*//B3LYP/6-31+G* level of calculation. The isomerization involves formation of a four-membered ring (**WM4V**), an open noncyclic chain (**WM4II**), and a five-membered ring (**WM4XII**) isomer as the intermediates. Out of the four transition states, the first one (**TS1**) is associated with four-membered ring formation (**WM4V**), made possible by hydrogen bond rotations. It resides about 1 kcal/

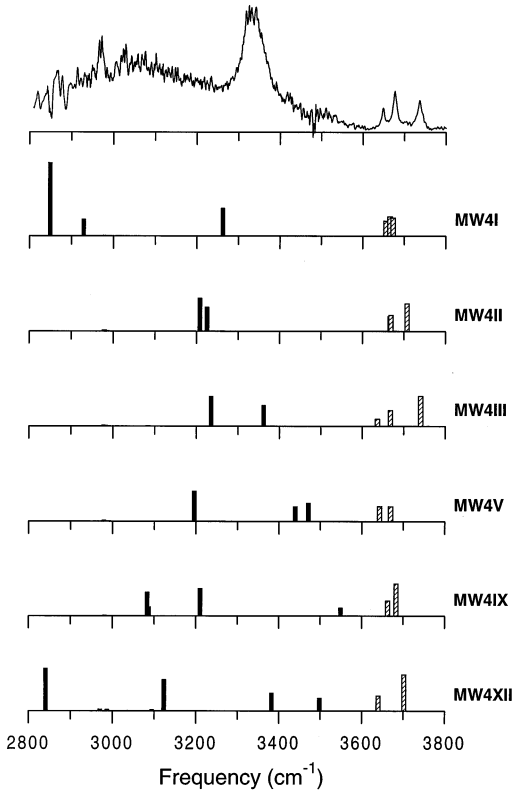

Figure 5. Power-normalized vibrational predissociation spectrum of $H^+(CH_3OH)_4H_2O$ generated by a supersonic expansion with a backing pressure of 30 Torr behind a corona-discharge nozzle. The spectrum was obtained by monitoring water loss and is compared to the calculated stick spectra for six representative isomers with structures depicted in Figure 4. Intensities of the free-OH stretches (slashed bars) have been amplified by a factor of 10 for clearer comparison to those of the bonded-OH stretches (solid bars).

mol (after zero-point energy corrections) above the potential minimum (**WM4I**). A similar height is found for the second barrier (**TS2**) with the ring opened prior to the subsequent five-membered ring formation. Figure 7 illustrates the structures (with the corresponding HB lengths given in angstroms) as well as the conversion sequence of the four transition states and three intermediates involved in this HB rearrangement process. As depicted in this figure, the structural reconstruction, $H_3O^+(CH_3OH)_4 \leftrightarrow CH_3OH_2^+(CH_3OH)_3H_2O$, is entangled with bond rotations, intracluster proton transfer, and hydrogen bond breaking and reforming, similar to that occurring in aqueous acids[2,3] and liquid methanol.[34,35]

A few points are worth noting for this structural reconstruction process (cf. Figure 7). First, the lowest energy pathway always involves ring closure with the bridging CH_3OH or H_2O molecule behaving like a double proton acceptor. The behavior persists in both the four-membered ring and five-membered ring formation (cf. **WM4V** and **WM4XII**). Second, whenever a new hydrogen bond is formed between two methanol molecules upon the ring closure, the hydrogen bond next to it would be ruptured in the subsequent ring-opening process. The ring opening and closing actions alternate, as the isomer climbs up the energy ladder. Third, the hydrogen bond making, breaking, and reforming are often accompanied by intermolecular proton transfer. This is readily seen for the transition from **WM4I** to **WM4V**, where the extra proton is originally taken by water but is given to the adjacent methanol molecule after the ring closure. Fourth, the structural reconstruction is made possible by large-amplitude motions of the methanol molecules, primarily through rotation of the intermolecular hydrogen bonds. Both the O−H···O bond angles and the interoxygen distances are substantially altered during the HB rearrangement processes.

An interesting and, perhaps, useful way to illustrate the HB rearrangement pathway in Figure 7 is to assess how the interoxygen separation (R_{oo}) between water and the charge center enlarges as the isomerization proceeds. From the figure, the separation is seen to increase from $R_{oo} = 0$ Å for **WM4I,** to $R_{oo} \approx 2.5$ Å for the intermediates states, and finally to $R_{oo} = 4.52$ Å for **WM4III**. It features a migration of the water molecule away form the ion core to the outer solvation shell of this protonated mixed water−methanol cluster. It should be noted that while the presently predicted isomerization barriers are all very low (less than 2.5 kcal/mol), the complexity of the water migration may substantially reduce the rate of the

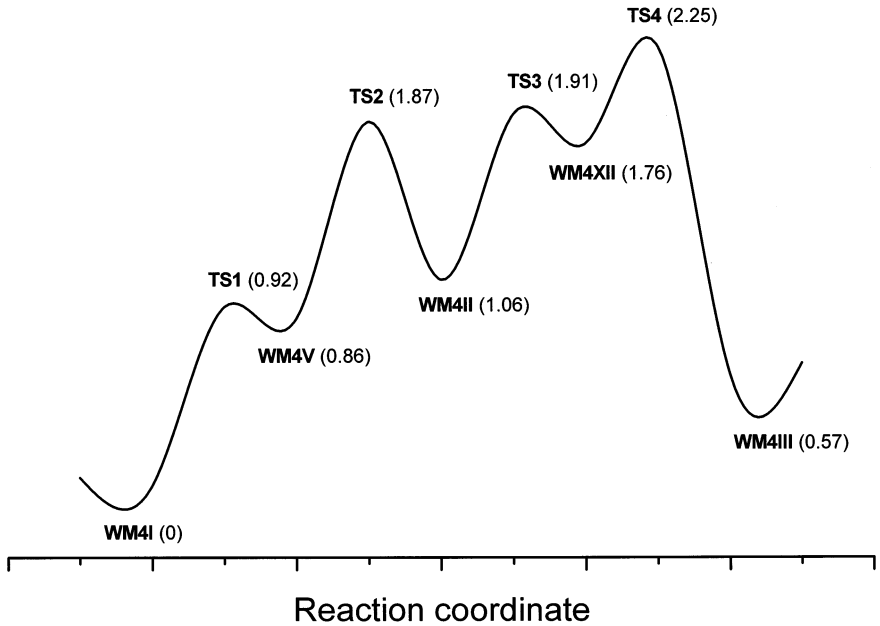

Figure 6. Energy profiles of the isomerization from **WM4I** to **WM4III**, predicted by the MP4/6-311+G*//B3LYP/6-31+G* level of computation for $H^+(CH_3OH)_4H_2O$. The numbers indicated are relative energies (kcal/mol) with respect to that of **WM4I**. The corresponding structures of five stable isomers and four transition states are given in Figure 7.

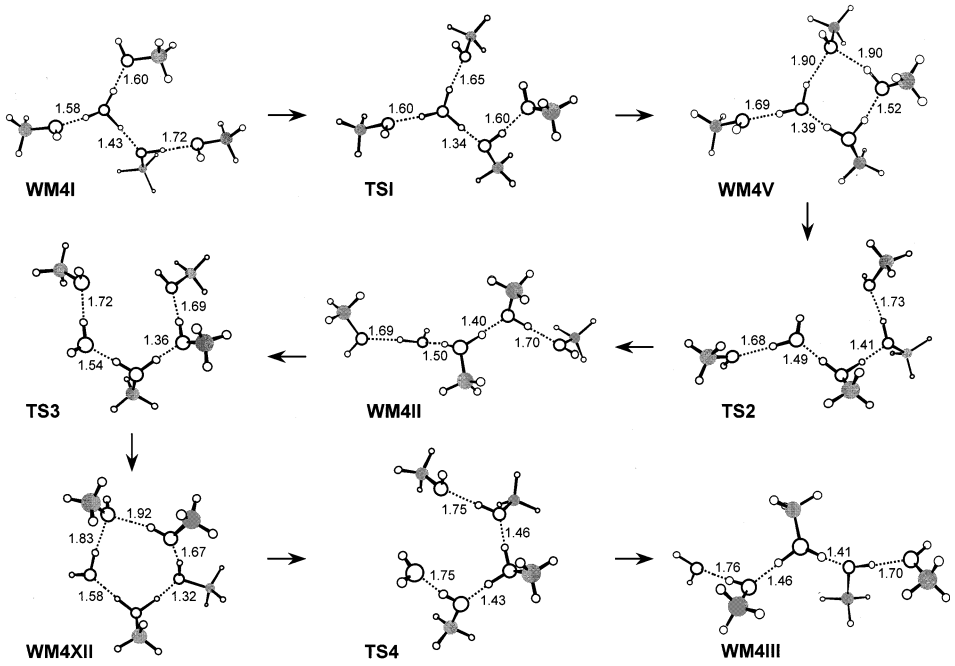

Figure 7. Rearrangements of hydrogen bonds leading to formation of isomer **WM4III** from **WM4I** for $H^+(CH_3OH)_4H_2O$. The C, O, and H atoms are denoted by large shaded, large open, and small open circles, respectively.

isomerization and, hence, the dissociation of isomer **WM4I** through the W-loss fragmentation channel.

As an alternative to the pathway described in Figure 6, the transition from **WM4I** to **WM4III** can go through the second HB rearrangement channel, which consists only of four-membered ring isomers as the intermediate states. The channel defines the pathway as **WM4I** → **WM4V** → **WM4II** → **WM4IX** → **WM4III** → **M4I** + H_2O. It involves formation of two four-membered ring intermediates bridged by one open noncyclic isomer along the way. Note that in the transition from **WM4II** to **WM4IX**, the ring-closing methanol molecule must act as a proton donor, which is not an energetically favored process. Moreover, since the four-membered ring structure **WM4IX** lies above other members of the cluster isomers by >2 kcal/mol (Table 1), a higher barrier must be overcome. A combination of these two factors makes this pathway less preferable than the first channel discussed earlier.

The energy landscape depicted in Figure 6 may give a proper explanation why isomer **WM4II** is not observed in the present experiment. Consider that when isomer **WM4II** is formed in the supersonic expansion, it can be easily converted to **WM4I** due to collisions with background H_2 gas, since only a small barrier (<1 kcal/mol) is involved in the conversion. Once the barrier (**TS2**) is overcome, it is a downhill process for **WM4II** to form the supersonically cooled **WM4I**. One may expect that a similar process can also occur for isomer **WM4III**. However, the barrier needed to cross over for this isomerization is significantly higher by ∼1 kcal/mol and, hence, the isomer can be found trapped at the bottom of the local potential well with higher probability and is experimentally observed.

Results of this investigation may provide new insight into the experimental observation of Garvey and co-workers,[24] who reported the detection of a magic cluster isomer for $H^+(CH_3OH)_9(H_2O)$. The isomer is remarkably symmetric, with the water molecule acting as an ion in the center of a half-clathrate structure. From a consideration of a need of breaking two hydrogen bonds and migration of the extra proton from water to the corresponding methanol oxygen side, the authors estimated that loss of water would require at least 10 kcal/mol more energy than loss of methanol for this cluster isomer. On the basis of the present analysis, we envision that less energy might be required than they estimated if the HB rearrangements depicted in this paper could also occur for this cluster isomer. Conceivably, in addition to energetics, the competition between the isomerization and the dissociation processes also governs the accessibility, and thus the branching, of these two (W-loss and M-loss) fragmentation channels.

IV. Conclusion

We have presented a case concerning rearrangements of hydrogen bonds in protonated water-containing clusters using $H^+(CH_3OH)_4H_2O$ as a model system. With water as the "tag" molecule, we trace its location within the cluster and analyze this case in detail. It is shown that the interconversion between H_3O^+- and $CH_3OH_2^+$-centered isomers (specifically, **WM4I** and **WM4III**) can occur rapidly at room temperature and the water molecule can move out of the methanol cage with a barrier height of less than 2.5 kcal/mol. The movement involves a series of ring-opening and -closing processes, transforming the structure through a four-membered ring, an open chain, and finally a five-membered ring isomer.

The analysis described in this work may be connected with the acid-catalyzed rearrangements of chemical bonds in protonated propene oxide[36] and water-assisted tautomerizations of protonated formamide and peptides,[37] both of which have been subjected to extensive theoretical investigations. Compared to the corresponding barriers with a height of ∼20 kcal/mol in molecular systems,[36] the barriers involved in the hydrogen-bonded cluster systems are lower by about 1 order of magnitude. We expect that the hydrogen bond rearrangement pathways presently attained for $H^+(CH_3OH)_4H_2O$ would be found in other water-containing cluster ions,[38] such as $H^+(H_2O)_n$ and $OH^-(H_2O)_n$, as well.[39] Similar analysis (both theoretical and experimental) can be made to delineate the mechanism of HB rearrangements in partial hydration of biological molecules in the gas phase.[40]

Acknowledgment. We thank the Chinese Petroleum Cooperation, the Academia Sinica, and the National Science Council (Grant No. NSC 90-2113-M-001-043) of Taiwan, R.O.C., for financial support of this work.

References and Notes

(1) Luzar, A.; Chandler, D. *Nature* **1996**, *379*, 55. Luzar, A. *Faraday Discuss.* **1996**, *103*, 29.

(2) Marx, D.; Tuckerman, M. E.; Hutter, J.; Parrinello, M. *Nature* **1999**, *397*, 601.

(3) Agmon, N. *Chem. Phys. Lett.* **1995**, *244*, 456. Agmon, N. *Chem. Phys. Lett.* **2000**, *319*, 247.

(4) Berry, R. S.; Fernandez, A.; Kostov, K. *Eur. Phys. J. D* **2001**, *16*, 47.

(5) Wales, D. J.; Doye, J. P. K.; Miller, M. A.; Mortenson, P. N.; Walsh, T. R. *Adv. Chem. Phys.* **2000**, *115*, 1.

(6) Wales, D. J. *J. Am. Chem. Soc.* **1993**, *115*, 11 180. Wales, D. J. *Science* **1996**, *271*, 925.

(7) Liu, K.; Loeser, J. G.; Elrod, M. J.; Host, B. C.; Rzepiela, J. A.; Pugliano, N.; Saykally, R. J. *J. Am. Chem. Soc.* **1994**, *116*, 3507. Liu, K.; Cruzan, J. D.; Saykally, R. J. *Science* **1996**, *271*, 929. Brown, M. G.; Viant, M. R.; McLaughlin, R. P.; Keoshian, C. J.; Michael, E.; Cruzan, J. D.; Saykally, R. J.; van der Avoird, A. *J. Chem. Phys.* **1999,** *111*, 7789.

(8) Keutsch, F. N.; Fellers, R. S.; Brown, M. G.; Viant, M. R.; Peterson, P. B.; Saykally, R. J. *J. Am. Chem. Soc.* **2001**, *123*, 3006.

(9) Wales, D. J.; Ohmine, I. *J. Chem. Phys.* **1993**, *98*, 7245. Wales, D. J.; Ohmine, I. *J. Chem. Phys.* **1993**, *98*, 7257.

(10) Wales, D. J. *J. Chem. Phys.* **1999**, *111*, 8429. Wales, D. J. *J. Chem. Phys.* **1999**, *110*, 10403.

(11) Yeh, L. I.-C.; Okumura, M.; Myers, J. D.; Price, J. M.; Lee, Y. T. *J. Chem. Phys.* **1989**, *91*, 7319. Yeh, L. I.-C.; Lee, Y. T.; Hougen, J. T. *J. Mol. Spectrosc.* **1994**, *164*, 473.

(12) Singer, S. J.; McDonald, S.; Ojamäe, L. *J. Chem. Phys.* **2000**, *112*, 710.

(13) Jiang, J. C.; Wang, Y.-S.; Chang, H.-C.; Lin, S. H.; Lee, Y. T.; Chang, H.-C. *J. Am. Chem. Soc.* **2000**, *122*, 1398.

(14) Wang, Y.-S.; Chang, H.-C.; Jiang, J. C.; Lin, S. H.; Lee, Y. T.; Chang, H.-C. *J. Am. Chem. Soc.* **1998**, *120*, 8777. Chang, H.-C.; Wang, Y.-S.; Lee, Y. T.; Chang, H.-C. *Int. J. Mass Spectrom.* **1998**, *180*, 91.

(15) Chang, H.-C.; Jiang, J. C.; Lin, S. H.; Lee, Y. T.; Chang, H.-C. *J. Phys. Chem. A* **1999**, *103*, 2941. Chang, H.-C.; Jiang, J. C.; Chang, H.-C.; Wang, L. R.; Lee, Y. T. *Isr. J. Chem.* **2000**, *39*, 231.

(16) Hahndorf, I.; Jiang, J. C.; Chang, H.-C.; Wu, C.-C.; Chang, H.-C. *J. Phys. Chem. A* **1999**, *103*, 8753.

(17) Chaudhuri, C.; Jiang, J. C.; Wang, X.; Lee, Y. T.; Chang, H.-C. *J. Chem. Phys.* **2000**, *112*, 7279.

(18) Meot-Ner, M. *J. Am. Chem. Soc.* **1986**, *108*, 6189.

(19) Kebarle, P.; Haynes, R. N.; Collins, J. G. *J. Am. Chem. Soc.* **1967**, *89*, 5753.

(20) Stace, A. J.; Shukla, A. K. *J. Am. Chem. Soc.* **1982**, *104*, 5314.

(21) Zhang, X.; Castleman, A. W., Jr. *J. Chem. Phys.* **1994**, *101*, 1157.

(22) Vaidyanathan, G.; Herron, W. J.; Garvey, J. F. *J. Phys. Chem.* **1993**, *97*, 7880. Herron, W. J.; Coolbaugh, M. T.; Vaidyanathan, G.; Garvey, J. F. *J. Am. Chem. Soc.* **1992**, *114*, 3684. Garvey, J. F.; Herron, W. J.; Vaidyanathan, G. *Chem. Rev.* **1994**, *94*, 1999.

(23) Karpas, Z.; Eiceman, G. A.; Harden, C. S.; Ewing, P. B. W.; Smith, R. G. *Org. Mass Spectrom.* **1994**, *29*, 159.

(24) Lyktey, M. M. Y.; DeLeon, R. L.; Shores, K. S.; Furlani, T. R.; Garvey, J. F. *J. Phys. Chem. A* **2000**, *104*, 5197.

(25) Wu, C.-C.; Jiang, J. C.; Boo, D. W.; Lin, S. H.; Lee, Y. T.; Chang, H.-C. *J. Chem. Phys.* **2000**, *112*, 176.

(26) Hunter, E. P. L.; Lias, S. G. *J. Phys. Chem. Ref. Data* **1998**, *27*, 413.

(27) Ichihashi, M.; Yamabe, J.; Murai, K.; Nonose, S.; Hirao, K.; Kondow, T. *J. Phys. Chem.* **1996**, *100*, 10050.

(28) Klots, C. E. *Z. Phys. D* **1991**, *20*, 105.

(29) Gaussian 98, Revision A.5, Frisch, M. J.; Trucks, G. W.; Schlegel, H. B.; Scuseria, G. E.; Robb, M. A.; Cheeseman, J. R.; Zakrzewski, V. G.; Montgomery, Jr., J. A.; Stratmann, R. E.; Burant, J. C.; Dapprich, S.; Millam, J. M.; Daniels, A. D.; Kudin, K. N.; Strain, M. C.; Farkas, O.; Tomasi, J.; Barone, V.; Cossi, M.; Cammi, R.; Mennucci, B.; Pomelli, C.; Adamo, C.; Clifford, S.; Ochterski, J.; Petersson, G. A.; Ayala, P. Y.; Cui, Q.; Morokuma, K.; Malick, D. K.; Rabuck, A. D.; Raghavachari, K.; Foresman, J. B.; Cioslowski, J.; Ortiz, J. V.; Stefanov, B. B.; Liu, G.; Liashenko, A.; Piskorz, P.; Komaromi, I.; Gomperts, R.; Martin, R. L.; Fox, D. J.; Keith, T.; Al-Laham, M. A.; Peng, C. Y.; Nanayakkara, A.; Gonzalez, C.; Challacombe, M.; Gill, P. M. W.; Johnson, B.; Chen, W.; Wong, M. W.; Andres, J. L.; Gonzalez, C.; Head-Gordon, M.; Replogle, E. S.; Pople, J. A. Gaussian, Inc., Pittsburgh, PA, 1998.

(30) Jiang, J. C.; Chang, H.-C.; Lee, Y. T.; Lin, S. H. *J. Phys. Chem. A* **1999**, *103*, 3123.

(31) Xantheas, S. S. *J. Chem. Phys.* **1995**, *102*, 4505.

(32) Jiang, J. C. unpublished results.

(33) The rotational conformers are not considered in the present calculations.

(34) Grunwald, E.; Jumper, C. F.; Meiboom, S. *J. Am. Chem. Soc.* **1962**, *84*, 4, 4664.

(35) Matsumoto, M.; Gubbins, K. E. *J. Chem. Phys.* **1990**, *93*, 1981.

(36) Coxon, J. M.; Maclagan, R. G. A. R.; Rauk, A.; Thorpe, A. J.; Whalen, D. *J. Am. Chem. Soc.* **1997**, *119*, 4712.

(37) Rodriquez, C. F.; Cunje, A.; Shoeib, T.; Chu, I. K.; Hopkinson, A. C.; Siu, K. W. M. *J. Phys. Chem. A* **2000**, *104*, 5023. Rodriquez, C. F.; Cunje, A.; Shoeib, T.; Chu, I. K.; Hopkinson, A. C.; Siu, K. W. M. *J. Am. Chem. Soc.* **2001**, *123*, 3006.

(38) Niedner-Schatteburg, G.; Bondybey, V. E. *Chem. Rev.* **2000**, *100*, 4059.

(39) Chaudhuri, C.; Wang, Y.-S.; Jiang, J. C.; Lee, Y. T.; Chang, H.-C.; Niedner-Schatteburg, G. *Mol. Phys.* **2001**, *99*, 1161.

(40) See, for example, Jarrold, M. F. *Acc. Chem. Res.* **1998,** *32*, 360.